Improving the Assembly Speed, Quality, and Tunability of Thin Conductive Multilayers

Forrest S. Gittleson, David J. Kohn, Xiaokai Li, and André D. Taylor*

Department of Chemical Engineering, Yale University, P.O. Box 208286, New Haven, Connecticut 06520-8286, United States

ABSTRACT

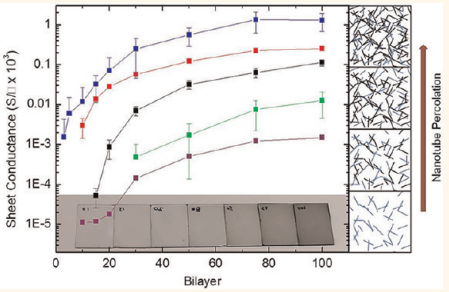

While inhomogeneous thin conductive films have been sought after for their flexibility, transparency, and strength, poor control in the processing of these materials has restricted their application. The versatile layer-by-layer assembly technique allows greater control over film deposition, but even this has been hampered by the traditional dip-coating method. Here, we employ a fully automated spin-spray layer-by-layer system (SSLbL) to rapidly produce high-quality, tunable multilayer films. With bilayer deposition cycle times as low as 13 s (~50% of previously reported) and thorough characterization of film conductance in the near percolation region, we show that SSLbL permits nanolevel control over film growth and efficient formation of a conducting network not available with other methods of multilayer deposition. The multitude of variables from spray time, to spin rate, to active drying available with SSLbL makes films generated by this technique inherently more tunable and expands the opportunity for optimization and application of composite multilayers. A comparison of several polymer—CNT systems deposited by both spin-spray and dip-coating exemplifies the potential of SSLbL assembly to allow for rapid screening of multilayer films. Ultrathin polymer—CNT multilayers assembled by SSLbL were also evaluated as lithium-ion battery electrodes, emphasizing the practical application of this technique.

KEYWORDS: layer-by-layer · conductive thin film · carbon nanotube · percolation · lithium-ion battery

Thin functional films have traditionally been produced by low-tech processes such as casting and dip-coating, but these methods are both slow and offer a low level of control over film properties. An alternative scheme is layer-by-layer assembly,[1−4] which involves the well-controlled sequential deposition of polyelectrolyte pairs to produce thin films with polymer multilayer architectures. Using the dip-coating method of layer-by-layer (LbL) assembly, deposition of a single bilayer (including polycation and polyanion) typically requires a minimum of 20 to 30 min.[5−7] Several studies have employed spray deposition[6,8−13] or dewetting[14] to reduce this cycle time to around one minute and have even automated the process.[15,16] Spin-coating of multilayer thin films has also shown a decrease in cycle time and a beneficial ordering of film components due to the shear forces applied during assembly.[17,18] The spin-spray layer-by-layer (SSLbL) assembly technique, first demonstrated by Merrill and Sun,[19] unites several of these processes as polyelectrolyte solutions are sequentially sprayed onto a rotating substrate. In addition to lower cycle times, SSLbL assembly has been shown to decrease material waste and enhance control over film thickness.

We report the development of an automated SSLbL film assembly apparatus that permits subsecond spray times to produce LbL films with cycle times ~50% shorter than previously reported (13 s *versus* 25 s reported by Merrill and Sun[19]). We demonstrate the ability to further reduce cycle times down to the subsecond range (*i.e.*, 0.8 s) for selected polymer systems. The SSLbL approach is advantageous in comparison to dip-coating because polyelectrolyte assembly is not limited by diffusion processes. High-speed substrate rotation, active drying at elevated temperatures, and the ability to considerably shorten rinse times with our system all serve to limit the contact time between the solution and the surface. Previous applications of spray-LbL have involved either low speed (*i.e.*, 10 rpm) vertical rotation[9] or a fixed orientation[6] of the substrate, which leads to the removal of excess solution by gravity; our apparatus eliminates this bottleneck. The result is that SSLbL-assembled multilayer films can be

* Address correspondence to andre.taylor@yale.edu.

Received for review November 11, 2011 and accepted April 19, 2012.

Published online April 20, 2012
10.1021/nn204384f

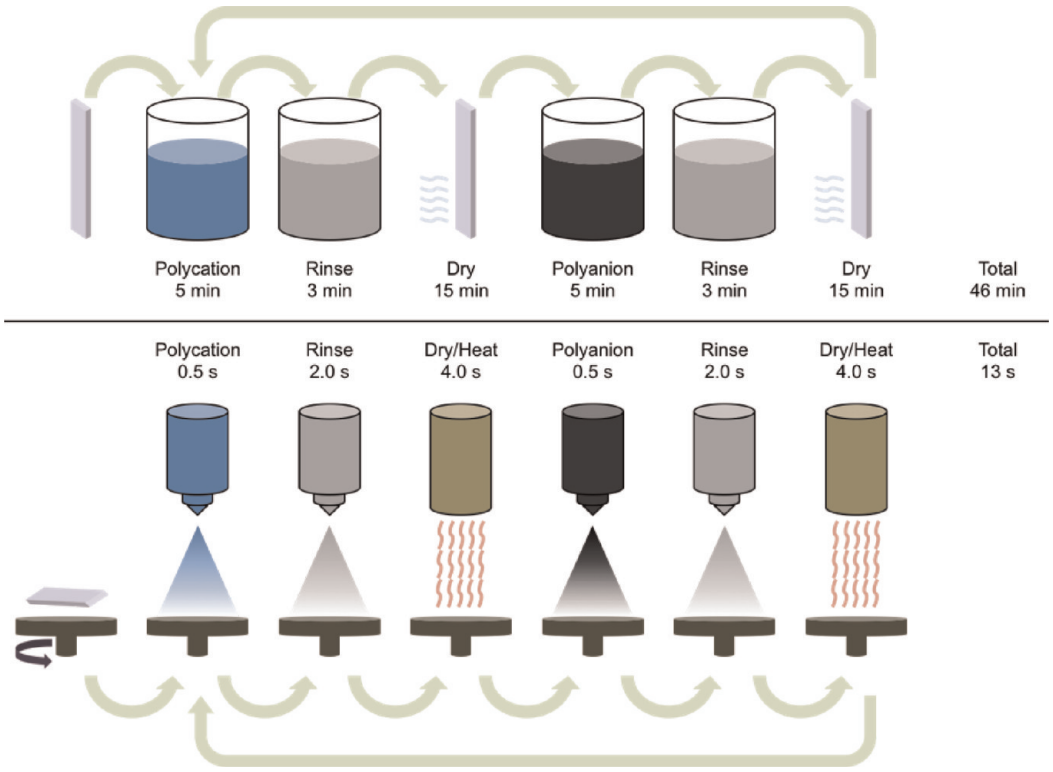

Figure 1. Schematic of dip-LbL (top) and SSLbL (bottom) processes and cycle times.

more easily and comprehensively tuned in thickness and other desired characteristics. Nanolevel control over deposition is achieved by adjusting variables including solution concentration, spray time, substrate spin rate, drying time, drying air flow, and temperature. The exceptional speed and tunability available with SSLbL make it inherently useful in the rapid screening of multicomponent polymer films for desired characteristics including conductance, strength, and stability. This is exemplified by the finding that films of equivalent sheet conductance that take 76 h to produce *via* dip-coating are generated in 54 min using SSLbL assembly.

Including carbon nanotubes in LbL films has been shown to produce thin films that are mechanically strong, stable, and most importantly conductive.[6,20−24] Here we use the SSLbL technique to demonstrate multilayer growth of several polymer−CNT composite films and report the effects of various parameters (*i.e.*, film thickness, polymer choice, nanotube content) on film conductance. We show that the SSLbL technique produces composite multilayers that are more uniform in conductance and more efficient in the use of carbon nanotubes to create a conducting network than those produced by the traditional dip-coating method. A high level of control over film conductance in the near percolation regime is also demonstrated due to nanotube layer stacking. These types of LbL composite films are particularly useful for electrochemical applications including batteries,[5,25−27] fuel cells,[28−32] solar cells,[20,21,33] and sensors.[22,34,35] Here, we demonstrate their use as electrode films for lithium-ion batteries. With the significant improvements in speed and control available with SSLbL, this versatile technique encourages the optimization and further application of functional multicomponent films.

RESULTS

Using the SSLbL apparatus, films of polyelectrolyte pairs [poly(styrene sulfonate) (PSS) + single-walled carbon nanotubes (SWNT)]/poly(vinyl alcohol) (PVA), [PSS + multiwalled carbon nanotubes (MWNT)]/PVA, (Nafion+SWNT)/polyethyleneimine (PEI), and (PSS+SWNT)/polyaniline (PANI) were deposited on cleaned glass slides or silicon wafers. The LbL formation mechanism was confirmed for each polymer system by spraying solutions of SWNT-containing polyelectrolyte with and without a counter-polymer. Without the counter-polymer, no film formation was observed (Figure S1 in the Supporting Information). For comparison, (PSS+SWNT)/PVA films were also assembled using the traditional dip-coating LbL (dip-LbL) method. Films of (PSS+SWNT)/PVA assembled by SSLbL employed the single cycle settings of 0.5 s spray of PVA, 2 s rinse, 4 s dry, 0.5 s spray of PSS+SWNT, 2 s rinse, and 4 s dry (giving a total cycle time of 13 s), while the dip-LbL cycle settings included a 5 min immersion in PVA solution, 3 min rinse, 15 min dry, 5 min immersion in PSS+SWNT solution, 3 min rinse, and 15 min dry (giving a total cycle time of 46 min) (Figure 1). The standard SSLbL procedure will be denoted

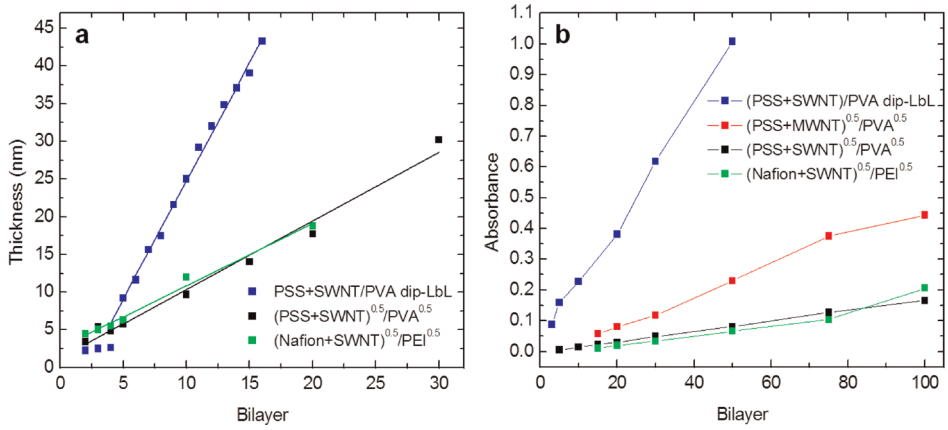

Figure 2. (a) Thickness of dip-LbL-assembled PSS+SWNT/PVA and SSLbL-assembled $(PSS+SWNT)^{0.5}/PVA^{0.5}$ and $(Nafion+SWNT)^{0.5}/PEI^{0.5}$ with best fit lines. (b) Absorbance of dip-LbL-assembled PSS+SWNT/PVA, $(PSS+SWNT)^{0.5}/PVA^{0.5}$, $(PSS+MWNT)^{0.5}/PVA^{0.5}$, and $(Nafion+SWNT)^{0.5}/PEI^{0.5}$ at 380 nm.

$(PSS+SWNT)^{0.5}/PVA^{0.5}$, with the rinse and dry times held constant unless otherwise noted. Film growth for both methods was analyzed by ellipsometry and UV−vis spectrophotometry, and film morphology by scanning electron microscopy (SEM) and atomic force microscopy (AFM).

We show in Figure 2a that film thickness per bilayer is nearly four times greater for dip-LbL-assembled films than for SSLbL-assembled films, consistent with a similar comparison between dip-LbL and spray-LbL made by Izquierdo *et al.*[6] The growth rate of the SSLbL-assembled (PSS+SWNT)/PVA film was approximately 0.8 nm/bilayer, while that of the dip-LbL-assembled (PSS+SWNT)/PVA was 3.1 nm/bilayer, exemplifying nanolevel control of thickness with SSLbL. This finding agrees with previous studies that have shown spin-coating to produce more compact, uniform LbL films than dip-coating.[17,18] A comparison of the thicknesses of (PSS+SWNT)/PVA and (Nafion+SWNT)/PEI films assembled by SSLbL shows that the growth rates are similar. We note that for films under five bilayers the dip-LbL method exhibits different growth characteristics than the SSLbL method. In dip-coating it is common to see negligible film growth for the first few layers until a stable coating of the substrate is achieved.[20] This phenomenon is observed in our dip-coated LbL films in contrast to those preliminary layers formed by SSLbL. This constant film growth for ultrathin SSLbL films without a precoat can be attributed to the active drying and spin-casting mechanisms that ensure good adhesion to the substrate. Conformal coverage of the substrate using SSLbL, even for low-bilayer films, has been confirmed and is reflected visually in Figure S2, where a gradient in film tone is shown across films of increasing bilayer number.

Nanotube content in $(PSS+SWNT)^{0.5}/PVA^{0.5}$, $(PSS+MWNT)^{0.5}/PVA^{0.5}$, $(Nafion+SWNT)^{0.5}/PEI^{0.5}$, and dip-LbL-assembled (PSS+SWNT)/PVA films of varying bilayers was also compared on the basis of absorbance at a wavelength of 380 nm, with the assumption that absorbance of the polymer is negligible (Figure 2b). The absorbance of SWNT in the (PSS+SWNT)/PVA and (Nafion+SWNT)/PVA systems for films of equal bilayer was similar, suggesting that the dispersion quality of SWNT in PSS and Nafion is comparable. This illustrates the exceptional control offered by SSLbL spray parameters despite the difference in the polymer system. The absorbance due to SWNT in dip-LbL-assembled films is significantly higher than for any of the SSLbL-assembled films, which can be attributed to differences in both thickness and morphology (Figure 3a,b). SSLbL-assembled (PSS+MWNT)/PVA films exhibit a higher absorbance per bilayer than similar films with SWNT, a finding that can be credited to both the larger diameter of the MWNT compared to SWNT and the better dispersion quality of the PSS+MWNT solution. (PSS+SWNT)/PANI multilayers could not be analyzed by this method since the characteristic emerald color of PANI would yield a non-negligible absorbance.

Figure 3 shows the distinct surface morphology of 30-bilayer films of each polymer−composite system studied. We attribute the difference in morphology between dip-LbL and SSLbL-assembled (PSS+SWNT)/PVA (Figure 3a,b) to the much higher growth rate of dip-coated LbL films shown previously and the effect of shear forces on the spinning substrate to produce denser and more uniform multilayers. AFM images of 15-bilayer films deposited on glass substrates are also shown in Figure S3 along with corresponding measurements of surface roughness (Table S1). Since roughness commonly increases with film thickness, it is reasonable to find that a dip-LbL-assembled film is rougher than an SSLbL-assembled film of the same number of bilayers. Percolating nanotube networks are evident in Figure 3b−d and account for the conductivity of these films. We note that the MWNTs in the (PSS+MWNT)/PVA system form a much denser network than SWNTs in the (PSS+SWNT)/PVA system,

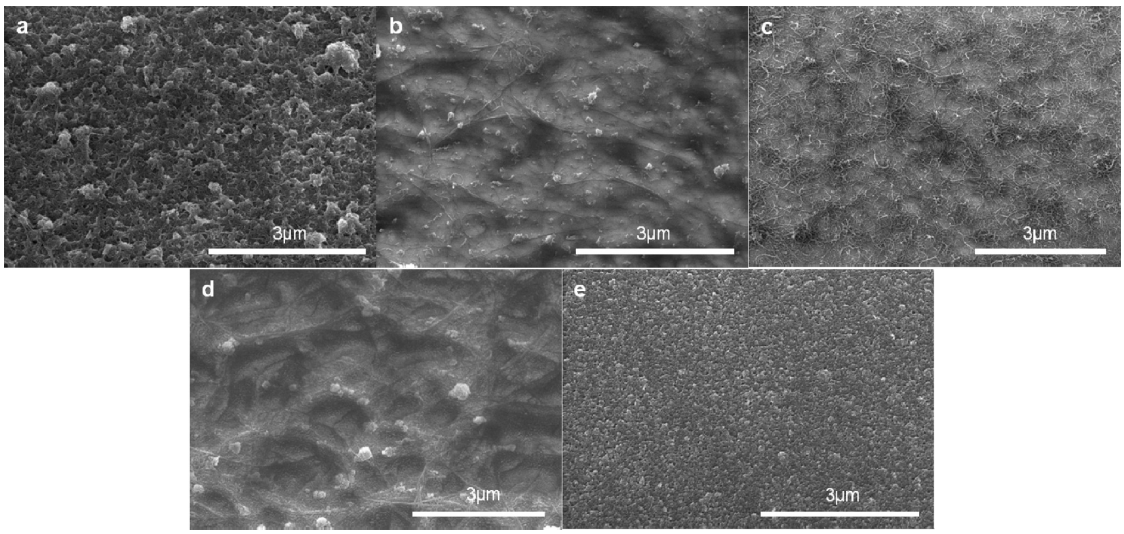

Figure 3. SEM surface morphology of (a) $[PSS+SWNT/PVA]_{30}$ by dip-LbL, (b) $[(PSS+SWNT)^{0.5}/PVA^{0.5}]_{30}$, (c) $[(PSS+MWNT)^{0.5}/PVA^{0.5}]_{30}$, (d) $[(Nafion+SWNT)^{0.5}/PEI^{0.5}]_{30}$, and (e) $[(PSS+SWNT)^{0.5}/PANI^{0.5}]_{30}$.

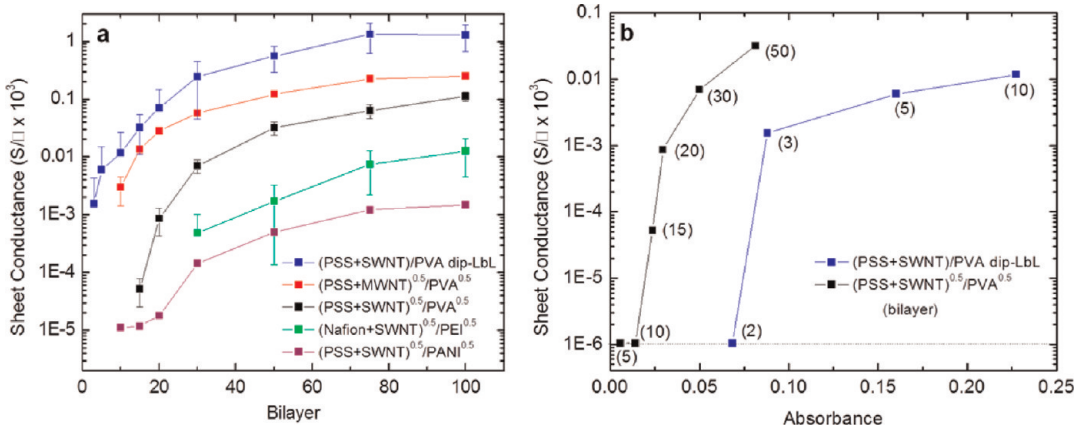

Figure 4. (a) Sheet conductance as a function of bilayer number in SSLbL- and dip-LbL-assembled films. (b) Percolation region for the formation of conducting nanotube networks in (PSS+SWNT)/PVA; dashed line indicates measurement threshold. For clarity, conductances that do not meet the measurement threshold are excluded from (a).

which we credit to better debundling and stability of MWNT in solution. The visual appearance of the nanotube network found in the (PSS+SWNT)/PVA and (Nafion+SWNT)/PEI films is similar, which corresponds well with the results for film thickness and absorbance. No nanotubes are apparent in the (PSS+SWNT)/PANI system due to the high concentration of PANI that covers the CNT (Figure 3e). The (PSS+SWNT)/PANI film is also quite rough in comparison to other SSLbL-assembled films (Table S1), a product of the morphology of the as-received PANI.

Carbon nanotube containing films have been noted for their potential use in optoelectronics, sensors, and electrodes due to the formation of a percolating nanotube network.[36,37] With nanolevel control, the SSLbL method is able to showcase a high-resolution correlation between sheet conductance and film thickness in the near percolation regime and during subsequent film growth (Figure 4), a result not seen in previous conductivity studies using dip-LbL. Superior control over conductivity is illustrated in the standard deviation of the sheet conductance for SSLbL-assembled (PSS+SWNT)/PVA films. Since these error values were calculated from five points evenly distributed across the film, we can conclude that the SSLbL method produces a more uniformly conductive film than the dip-LbL method.

From our screening of several polymer−CNT systems using the SSLbL method we find that the choice of polymer pairs has a large effect on the sheet conductance of these films. While the (Nafion+SWNT)/PEI system grows at a similar rate to (PSS+SWNT)/PVA, its conductance (Figure 4a) appears much lower. Since the conductivity of a nanotube network is a function of junction distance,[38] we attribute the significantly lower conductance in (Nafion+SWNT)/PEI films to the formation of a less densely packed SWNT network, but not necessarily a less densely packed bulk film.

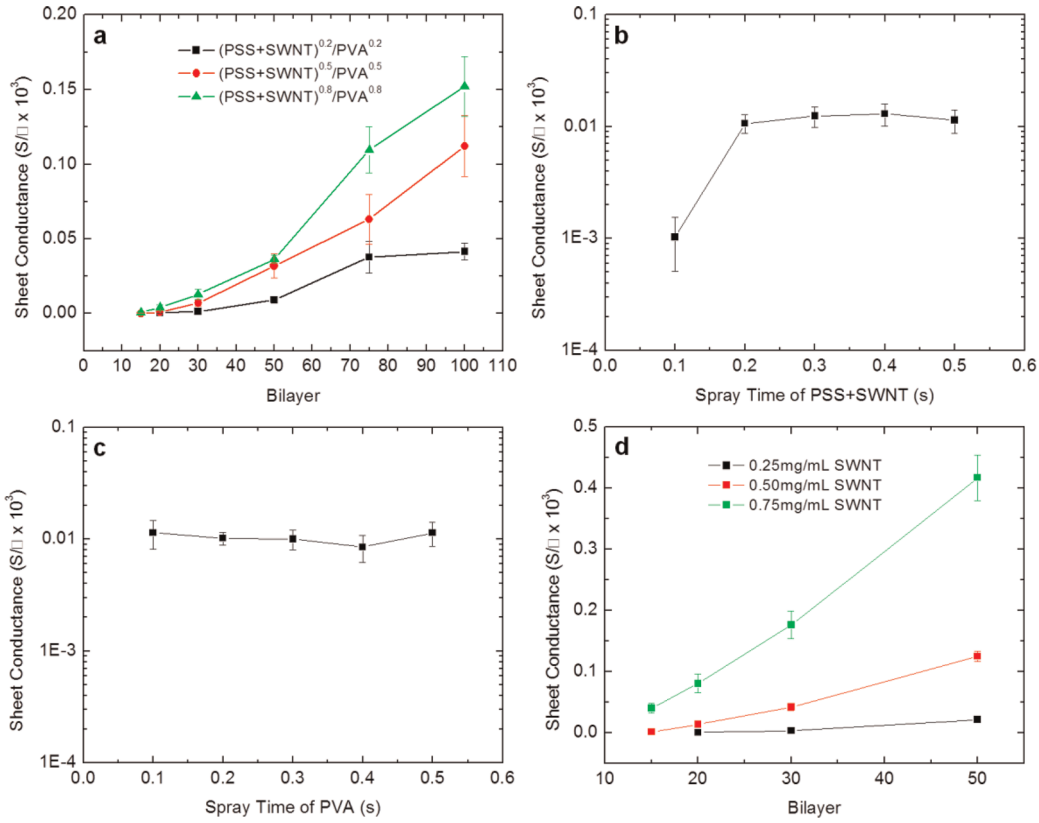

Figure 5. (a) Effect of polyelectrolyte spray time on sheet conductance for (PSS+SWNT)/PVA. (b) Effect of PSS+SWNT spray time on sheet conductance in $[(PSS+SWNT)^{x}/PVA^{0.5}]_{30}$. (c) Effect of PVA spray time on sheet conductance in $[(PSS+SWNT)^{0.5}/PVA^{x}]_{30}$. (d) Effect of SWNT concentration on sheet conductance for $(PSS+SWNT)^{0.5}/PVA^{0.5}$.

This distinction may be the result of increased porosity in Nafion-containing films or differences in polymer wrapping of SWNT. We also see in Figure 4a that the (PSS+MWNT)/PVA system exhibits a larger conductance per bilayer compared with (PSS+SWNT)/PVA, which can be attributed to the increased concentration of nanotubes and greater debundling.

For ultrathin films, it is also apparent that the dip-LbL and SSLbL processes lead to films with different percolation thresholds (Figure 4b). Despite the fact that SSLbL-assembled (PSS+SWNT)/PVA films are thinner and contain fewer nanotubes in the low-bilayer percolation regime than those assembled by dip-LbL, they are comparable in sheet conductance. With decreased layer thicknesses and improved film compactness, we believe that through-plane interaction between nanotube-containing layers in SSLbL-assembled films is more favorable to electrical conduction than in dip-LbL films. In other words, where "fuzzy" layers are beneficial, as in polymer composites, SSLbL can provide better bilayer blending. This finding is a product of the decreased bilayer thickness with SSLbL, wherein SWNTs have a diameter of 1−2 nm (greater than the average bilayer thickness of 0.8 nm), suggesting significant overlap. Our results also imply that the efficiency of use of high-value components such as nanotubes can be improved using the SSLbL method.

The exceptional tunability of SSLbL-assembled films is a product of the many variables available for optimization. Subsecond spray is an especially powerful tool for tuning conductance. With all else held constant, (PSS+SWNT)/PVA films with 0.2, 0.5, and 0.8 s polyelectrolyte and SWNT spray times illustrate the high resolution of control SSLbL permits (Figure 5a). The effectiveness of the rinse and spin mechanisms in removing excess polyelectrolyte from the substrate is illustrated in Figure 5b,c. Holding the PVA spray time constant at 0.5 s and varying the PSS+SWNT spray time from 0.1 s to 0.5 s reveals that after the maximum amount of CNT is deposited on the surface there is no improvement in conductance from increasing the amount of solution sprayed. This result is particularly valuable for reducing material waste, especially of high-cost colloids such as SWNTs and catalysts. Conversely, holding the PSS+SWNT spray time constant at 0.5 s and varying the PVA spray time from 0.1 s to 0.5 s reveals that there is no penalty from spraying excesses of nonconductive polymers due to the removal mechanism. Varying both spray times in tandem as in Figure 5a, however, leads to a multiplier effect on conductance, which allows the production of films with highly tunable conductivities. This result should allow further optimization of process times and a reduction in material waste. We also report the ability

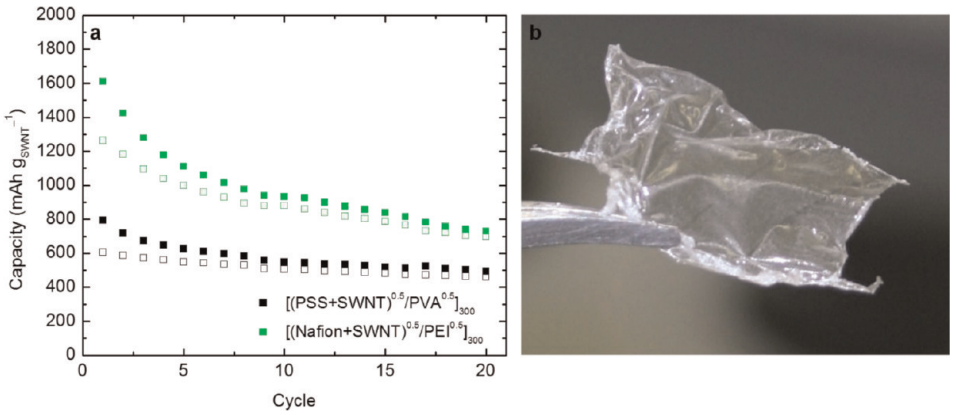

Figure 6. (a) Battery cycling of SSLbL-assembled films on Celgard separator *vs* Li, lithiation capacity is indicated by closed squares and delithiation capacity by open squares. (b) Freestanding [PAA$^{0.2}$/PEO$^{0.2}$]$_{1500}$.

to control conductance based on upstream solution preparation. Varying the SWNT concentration in PSS solution yields a direct correlation between the amount of nanotubes being sprayed and the conductance of the resulting film (Figure 5d). The potential to fine-tune LbL film properties shown here results from the unique ability of the SSLbL method to closely control material deposition though spray parameters, residence times, and solution concentrations.

We demonstrate the practical application of SSLbL-assembled polymer–CNT films through an evaluation of their anodic capacity in a lithium-ion battery half-cell *versus* lithium foil. It has been shown previously that SWNT acts as a lithium intercalation compound in a manner similar to graphite, albeit with more favorable stoichiometry and a better capacity (approximately 1100 *versus* 372 mAh/g for graphite).[39] Toward the scalable fabrication of multifunctional composite electrodes,[40] several studies have demonstrated the use of SWNT-containing anodes,[39–42] while others have used the LbL technique to generate active battery electrodes.[26,27] To our knowledge, however, we report the first evaluation of SWNT-containing LbL polymer–composite films as lithium-ion battery anodes. We compared SSLbL-assembled films of [(PSS+SWNT)$^{0.5}$/PVA$^{0.5}$]$_{300}$ and [(Nafion+SWNT)$^{0.5}$/PEI$^{0.5}$]$_{300}$ (each generated in 65 min) to determine which factors affect charge/discharge capacity. All films were galvanostatically cycled at 37 mA/g_{SWNT} for 20 cycles to gauge stability and capacity (Figure 6a). Though we found that the (PSS+SWNT)/PVA and (Nafion+SWNT)/PEI films have roughly the same nanotube content per bilayer, the cycling performance was quite distinct. The (Nafion+SWNT)/PEI system performs better after 20 cycles than the (PSS+SWNT)/PVA system (delithiation capacities are 699 and 460 mAh/g_{SWNT}, respectively). Despite the fact that (PSS+SWNT)/PVA films show a significantly higher sheet conductance than those of (Nafion+SWNT)/PEI, the difference in performance may be attributed to the enhanced ion conductivity and stability of Nafion.[43,44] Because these films are significantly thinner (~250 nm) than most conventional lithium-ion battery electrodes (*i.e.*, 100 μm), we have neglected the thickness of the SSLbL-assembled films as a factor in performance, believing that they are thin enough so as to not appreciably hinder ion transport with the liquid electrolyte. Further study of ultrathin LbL polymer–CNT electrodes for lithium-ion batteries is ongoing.

In addition to the evaluation of battery performance, we have assembled all-polymer films of poly(acrylic acid) (PAA)/poly(ethylene oxide) (PEO) and PSS/PANI by SSLbL, which have applications in batteries (as polymer electrolytes) and fuel cells (as catalyst layer ionomers), respectively.[31,34,45] Fully freestanding 1500-bilayer PAA/PEO (Figure 6b) and (PAA+SWNT)/PEO films were assembled using the SSLbL apparatus with cycle times of 0.8 s, minimizing the drying time. Having previously demonstrated dip-LbL-assembled films in fuel cell membrane electrode assemblies,[28,32] we believe that the SSLbL technique can also be applied to the rapid production of even higher quality fuel cell electrodes.

CONCLUSION

Here we have demonstrated a novel technique for rapidly building LbL films with a greater level of control than previously available. Employing subsecond spray times and active drying of the substrate, we generated highly tunable ultrathin polymer–composite films. The polymer–CNT systems used showcase the versatility of this approach as well as indicate the potential for rapid screening and further optimization with SSLbL. Comparisons to the conventional dip-coating method of film assembly show that greater film uniformity and deposition efficiency can be obtained by this method. SSLbL-assembled films with integrated CNTs were characterized, yielding a better correlation between LbL film growth and conductance than previously seen for these systems. Additionally, the application of LbL

polymer−CNT films as electrodes in lithium-ion batteries has been demonstrated for the first time, lending insights into the future development of ultrathin battery electrodes and ion conductive binders. The SSLbL technique is widely applicable to fundamental research and application of thin films, with specific opportunities available in energy conversion and storage.

METHODS

Spin-Spray Layer-by-Layer System. The SSLBL apparatus (Figure S6) consists of three gravity-fed 1/4 in. JAUMCO round spray setup sprayers from Spraying Systems Co. directed toward a spin coater (Specialty Coating Systems 6800 model) with a vacuum chuck to hold the substrate in place. The enclosure includes an inlet for the active heating element that directs heated air at the substrate and a negatively pressurized vent as well as a port for solutions. Convection within the enclosure is ensured with inlets and outlets of opposite pressures. Several control programs were written using Labview software that communicate with a National Instruments CompactRIO controller. Sprayers are actuated using solenoid valves from Parker Hannifin Co.

Materials. Poly(styrene sulfonate) (MW 1 000 000), polyethylenimine (MW 25 000), poly(vinyl alcohol), and polyaniline (MW 20 000) were purchased from Sigma-Aldrich Co. Poly(acrylic acid) (MW 50 000) and poly(ethylene oxide) (MW 4 000 000) were purchased from Polysciences Inc. A solution of 10 wt % Nafion (Dupont DE 1021) was purchased from Ion Power Inc. High -purity MWNTs were obtained from SouthWest NanoTechnologies (SMW 100). SWNTs (90% purity) were purchased from Cheaptubes Inc. (Raman spectra seen in Figure S7).

Solution Preparation. All polymers were dissolved or diluted in Milli-Q deionized (DI) water. Polyelectrolyte dispersions containing CNT were bath sonicated for 3 h, tip sonicated for 45 min, and centrifuged at 3000 rpm for 1.5 h to produce a stable dispersion. For the PSS+SWNT solution, there was significant loss of nanotubes during centrifugation. Minimal loss of CNTs was observed following centrifugation for solutions containing MWNT. Typical CNT solutions consisted of 0.5 mg/mL CNT in aqueous solutions of 1% PSS or 0.25% Nafion. PANI solutions were prepared in a manner similar to that found in Cheung *et al.*[46] The pH of solutions was adjusted using HCl and NaOH. PVA (10 mM) and high-concentration PANI solutions were adjusted to pH 2.8. Nafion and PEI solutions were adjusted to pH 8.5. PSS+SWNT solutions were not pH adjusted, except when paired with PANI, when they adjusted to pH 2.8.

Film Deposition. Glass slides were cleaned for 1 h by immersion in piranha solution consisting of 3:1 by volume of concentrated H_2SO_4 and H_2O_2, respectively. Cleaned slides were stored in DI water until LbL deposition. Substrates for battery electrodes consisted of Celgard 2325 porous separators stretched on aluminum foil. Deposition using the SSLbL apparatus involved spinning the substrate on a vacuum chuck at 3000 rpm (in agreement with Merrill and Sun[19]) while solutions were sprayed. A typical bilayer was assembled using a spray/dry procedure of polycation, rinse, dry, polyanion, rinse, dry. Polyelectrolyte spray times were either 0.2, 0.5, or 0.8 s. DI rinse water adjusted to match the pH of the polycation was typically sprayed for 2 s except in the case of films deposited on Celgard separators, for which rinse times were limited to 1 s. Dry times were maintained at 4 s to ensure complete drying between layers. The temperature of the heating element was kept constant, corresponding to a substrate temperature of approximately 40 °C.

Deposition by dip-LbL was conducted using a nanoStrata Inc. StratoSequence VI slide stainer in which glass substrates were dipped in polyelectrolytes for 5 min followed by three 1 min rinsing steps. Polyelectrolyte solutions were replaced after every 30 bilayers to limit the effect of cross contamination. Rinse water was replaced after each bilayer. For films containing SWNT, a 15 min drying step was added, which involved passing air over the film.

Characterization. Resistivity measurements were obtained using a Keithey 2400 SourceMeter and a Signatone four-point probe. Five measurements were taken across the surface at defined distances from the center of the substrate (Figure S5). Absorbance measurements were taken using a Hewlett-Packard UV−vis spectrophotometer, and comparisons were made using absorbance values at a wavelength of 380 nm. Absorbances for dip-LbL-assembled films were halved to account for film growth on both sides of the glass substrate. Film thicknesses were obtained by ellipsometry from samples deposited on silicon wafers. A Cauchy fit model with a refractive index of 1.435 was used to analyze the data. Visual characterization of films employed a Hitachi SU-70 scanning electron microscope and a Veeco Dimension 5000 atomic force microscope.

Battery cells were assembled in a Teflon Swagelok cell with stainless steel electrode plates. SSLbL-assembled films on Celgard separators were cut in circles with an area of 0.97 cm^2 and placed face down against the stainless steel current collector. A second Celgard separator was placed on top followed by lithium foil and several drops of 1 M $LiPF_6$ in 1:1 ethylene carbonate/dimethyl carbonate solvent. Cells were allowed to age for at least 12 h before cycling. Galvanostatic cycling of 300 bilayer films was conducted using a Biologic VSP potentiostat for 20 cycles at 11.16 μA. Capacity values were based on an assumed loading of ~10% SWNT, which is consistent with previous reports[20] as well as our own TGA analysis.

Conflict of Interest: The authors declare no competing financial interest.

Acknowledgment. We thank M. Rooks and the Yale Institute for Nanoscience and Quantum Engineering for assistance with AFM and SEM training and the Pfefferle and Haller groups for assistance with Raman spectroscopy. We also thank E. Jackson for guidance in designing the electronics of the SSLbL apparatus. We are grateful to W. Johnson and B. Redden of Armstrong Atlantic State University for assistance with CAD renderings and discussions involving the design of the SSLbL apparatus. We recognize the generous donation of CNT materials by SouthWest NanoTechnologies and acknowledge that support for this work came from the Semiconductor Research Corporation 2011-RJ-21516 and National Science Foundation NSF-CBET-0954985 CAREER Award.

Supporting Information Available: The Supporting Information provides evidence of the SSLbL growth mechanism (Figure S1) as well as visual indications of the growth and conformal coverage of the films deposited using the SSLbL method (Figure S2). AFM images and roughness calculations (Figure S3 and Table S1) for SSLbL films of different polymer systems are also shown. Figure S4 illustrates the radially dependent nature of sheet resistance in SSLbL-assembled films. A visual aid for understanding the position of resistance measurements across a typical thin film is presented (Figure S5). Also shown are the design of the SSLbL apparatus (Figure S6) and Raman spectra of the SWNT material used throughout this work (Figure S7). Finally, we provide a table of solution spray volumes that correspond to differing spray times (Figure S8) and an additional discussion on the data presented in Figure 5b,c (Figure S9). This material is available free of charge *via* the Internet at http://pubs.acs.org.

REFERENCES AND NOTES

1. Ariga, K.; Hill, J. P.; Ji, Q. Layer-by-Layer Assembly As a Versatile Bottom-Up Nanofabrication Technique for Exploratory Research and Realistic Application. *Phys. Chem. Chem. Phys.* **2007**, *9*, 2319–2340.
2. Decher, G. Fuzzy Nanoassemblies: Toward Layered Polymeric Multicomposites. *Science* **1997**, *277*, 1232–1237.

3. Decher, G.; Hong, J. D.; Schmitt, J. Buildup of Ultrathin Multilayer Films by a Self-Assembly Process: III. Consecutively Alternating Adsorption of Anionic and Cationic Polyelectrolytes on Charged Surfaces. *Thin Solid Films* **1992**, *210/211*, 831–835.
4. Hammond, P. T. Engineering Materials Layer-by-Layer: Challenges and Opportunities in Multilayer Assembly. *AIChE J.* **2011**, *57*, 2928–2940.
5. DeLongchamp, D. M.; Hammond, P. T. Highly Ion Conductive Poly(Ethylene Oxide)-based Solid Polymer Electrolytes from Hydrogen Bonding Layer-by-Layer Assembly. *Langmuir* **2004**, *20*, 5403–5411.
6. Izquierdo, A.; Ono, S. S.; Voegel, J.-C.; Schaaf, P.; Decher, G. Dipping Versus Spraying: Exploring the Deposition Conditions for Speeding Up Layer-by-Layer Assembly. *Langmuir* **2005**, *21*, 7558–7567.
7. Farhat, T. R.; Hammond, P. T. Fabrication of a "Soft" Membrane Electrode Assembly Using Layer-by-Layer Technology. *Adv. Funct. Mater.* **2006**, *16*, 433–444.
8. Cini, N.; Tulun, T.; Decher, G.; Ball, V. Step-by-Step Assembly of Self-patterning Polyelectrolyte Films Violating (Almost) All Rules of Layer-by-Layer Deposition. *J. Am. Chem. Soc.* **2010**, *132*, 8264–8265.
9. Krogman, K. C.; Zacharia, N. S.; Schroeder, S.; Hammond, P. T. Automated Process for Improved Uniformity and Versatility of Layer-by-Layer Deposition. *Langmuir* **2007**, *23*, 3137–3141.
10. Krogman, K. C.; Lowery, J. L.; Zacharia, N. S.; Rutledge, G. C.; Hammond, P. T. Spraying Asymmetry into Functional Membranes Layer-by-Layer. *Nat. Mater.* **2009**, *8*, 512–518.
11. Krogman, K. C.; Lyon, K. F.; Hammond, P. T. Metal Ion Reactive Thin Films Using Spray Electrostatic LbL Assembly. *J. Phys. Chem. B* **2008**, *112*, 14453–14460.
12. Ashcraft, J. N.; Argun, A. A.; Hammond, P. T. Structure-Property Studies of Highly Conductive Layer-by-Layer Assembled Membranes for Fuel Cell PEM Applications. *J. Mater. Chem.* **2010**, *20*, 6250–6257.
13. Schlenoff, J. B.; Dubas, S. T.; Farhat, T. Sprayed Polyelectrolyte Multilayers. *Langmuir* **2000**, *16*, 9968–9969.
14. Shim, B. S.; Podsiadlo, P.; Lilly, D. G.; Agarwal, A.; Lee, J.; Tang, Z.; Ho, S.; Ingle, P.; Paterson, D.; Lu, W.; Kotov, N. A. Nanostructured Thin Films Made by Dewetting Method of Layer-by-Layer Assembly. *Nano Lett.* **2007**, *7*, 3266–3273.
15. Nogueira, G. M.; Banerjee, D.; Cohen, R. E.; Rubner, M. F. Spray-Layer-by-Layer Assembly Can More Rapidly Produce Optical-Quality Multistack Heterostructures. *Langmuir* **2011**, *27*, 7860–7867.
16. Fukao, N.; Kyung, K.-H.; Fujimoto, K.; Shiratori, S. Automatic Spray-LBL Machine Based on in-Situ QCM Monitoring. *Macromolecules* **2011**, *44*, 2964–2969.
17. Vozar, S.; Poh, Y.-C.; Serbowicz, T.; Bachner, M.; Podsiadlo, P.; Qin, M.; Verploegen, E.; Kotov, N.; Hart, A. J. Automated Spin-assisted Layer-by-Layer Assembly of Nanocomposites. *Rev. Sci. Instrum.* **2009**, *80*, 023903.
18. Cho, J.; Char, K.; Hong, J.-D.; Lee, K.-B. Fabrication of Highly Ordered Multilayer Films Using a Spin Self-Assembly Method. *Adv. Mater.* **2001**, *13*, 1076–1078.
19. Merrill, M. H.; Sun, C. T. Fast, Simple and Efficient Assembly of Nanolayered Materials and Devices. *Nanotechnology* **2009**, *20*, 075606.
20. Shim, B. S.; Tang, Z.; Morabito, M. P.; Agarwal, A.; Hong, H.; Kotov, N. A. Integration of Conductivity, Transparency, and Mechanical Strength into Highly Homogeneous Layer-by-Layer Composites of Single-walled Carbon Nanotubes for Optoelectronics. *Chem. Mater.* **2007**, *19*, 5467–5474.
21. Shim, B. S.; Zhu, J.; Jan, E.; Critchley, K.; Kotov, N. A. Transparent Conductors from Layer-by-Layer Assembled SWNT Films: Importance of Mechanical Properties and a New Figure of Merit. *ACS Nano* **2010**, *4*, 3725–3734.
22. Loh, K. J.; Kim, J.; Lynch, J. P.; Kam, N. W. S.; Kotov, N. A. Multifunctional Layer-by-Layer Carbon Nanotube–Polyelectrolyte Thin Films for Strain and Corrosion Sensing. *Smart Mater. Struct.* **2007**, *16*, 429–438.
23. Olek, M.; Ostrander, J.; Jurga, S.; Möhwald, H.; Kotov, N.; Kempa, K.; Giersig, M. Layer-by-Layer Assembled Composites from Multiwall Carbon Nanotubes with Different Morphologies. *Nano Lett.* **2004**, *4*, 1889–1895.
24. Mamedov, A. A.; Kotov, N. A.; Prato, M.; Guldi, D. M.; Wicksted, J. P.; Hirsch, A. Molecular Design of Strong Single-Wall Carbon Nanotube/Polyelectrolyte Multilayer Composites. *Nat. Mater.* **2002**, *1*, 190–194.
25. Lee, S. W.; Kim, B.-S.; Chen, S.; Shao-Horn, Y.; Hammond, P. T. Layer-by-Layer Assembly of All Carbon Nanotube Ultrathin Films for Electrochemical Applications. *J. Am. Chem. Soc.* **2009**, *131*, 671–679.
26. Lee, S. W.; Yabuuchi, N.; Gallant, B. M.; Chen, S.; Kim, B.-S.; Hammond, P. T.; Shao-Horn, Y. High-Power Lithium Batteries from Functionalized Carbon-Nanotube Electrodes. *Nat. Nanotechnol.* **2010**, *5*, 531–537.
27. Nam, K. T.; Kim, D.-W.; Yoo, P. J.; Chiang, C.-Y.; Meethong, N.; Hammond, P. T.; Chiang, Y.-M.; Belcher, A. M. Virus-Enabled Synthesis and Assembly of Nanowires for Lithium Ion Battery Electrodes. *Science* **2006**, *312*, 885–888.
28. Taylor, A. D.; Michel, M.; Sekol, R. C.; Kizuka, J. M.; Kotov, N. A.; Thompson, L. T. Fuel Cell Membrane Electrode Assemblies Fabricated by Layer-by-Layer Electrostatic Self-Assembly Techniques. *Adv. Funct. Mater.* **2008**, *18*, 3003–3009.
29. Daiko, Y.; Katagiri, K.; Yazawa, T.; Matsuda, A. Thickness Dependences of Proton Conductivity for Ultrathin Nafion Multilayers Prepared via Layer-by-Layer Assembly. *Solid State Ionics* **2010**, *181*, 197–200.
30. Michel, M.; Ettingshausen, F.; Scheiba, F.; Wolz, A.; Roth, C. Using Layer-by-Layer Assembly of Polyaniline Fibers in the Fast Preparation of High Performance Fuel Cell Nanostructured Membrane Electrodes. *Phys. Chem. Chem. Phys.* **2008**, *10*, 3796–3801.
31. Wolz, A.; Zils, S.; Michel, M.; Roth, C. Structured Multilayered Electrodes of Proton/Electron Conducting Polymer for Polymer Electrolyte Membrane Fuel Cells Assembled by Spray Coating. *J. Power Sources* **2010**, *195*, 8162–8167.
32. Michel, M.; Taylor, A.; Sekol, R.; Podsiadlo, P.; Ho, P.; Kotov, N. High-Performance Nanostructured Membrane Electrode Assemblies for Fuel Cells Made by Layer-By-Layer Assembly of Carbon Nanocolloids. *Adv. Mater.* **2007**, *19*, 3859–3864.
33. Hong, T.-K.; Lee, D. W.; Choi, H. J.; Shin, H. S.; Kim, B.-S. Transparent, Flexible Conducting Hybrid Multilayer Thin Films of Multiwalled Carbon Nanotubes with Graphene Nanosheets. *ACS Nano* **2010**, *4*, 3861–3868.
34. Lutkenhaus, J. L.; Hammond, P. T. Electrochemically Enabled Polyelectrolyte Multilayer Devices: From Fuel Cells to Sensors. *Soft Matter* **2007**, *3*, 804–816.
35. Srivastava, S.; Kotov, N. A. Composite Layer-by-Layer (LbL) Assembly with Inorganic Nanoparticles and Nanowires. *Acc. Chem. Res.* **2008**, *41*, 1831–1841.
36. Hu, L.; Hecht, D. S.; Grüner, G. Percolation in Transparent and Conducting Carbon Nanotube Networks. *Nano Lett.* **2004**, *4*, 2513–2517.
37. Kyrylyuk, A. V.; Hermant, M. C.; Schilling, T.; Klumperman, B.; Koning, C. E.; Van der Schoot, P. Controlling Electrical Percolation in Multicomponent Carbon Nanotube Dispersions. *Nat. Nanotechnol.* **2011**, *6*, 364–369.
38. Fuhrer, M. S.; Nygard, J.; Shih, L.; Forero, M.; Yoon, Y.-G.; Mazzoni, M. S. C.; Choi, H. J.; Ihm, J.; Louie, S. G.; Zettl, A.; McEuen, P. L. Crossed Nanotube Junctions. *Science* **2000**, *288*, 494–497.
39. Landi, B. J.; Ganter, M. J.; Cress, C. D.; DiLeo, R. A.; Raffaelle, R. P. Carbon Nanotubes for Lithium Ion Batteries. *Energy Environ. Sci.* **2009**, *2*, 638–654.
40. Li, X.; Gittleson, F.; Carmo, M.; Sekol, R. C.; Taylor, A. D. Scalable Fabrication of Multifunctional Freestanding Carbon Nanotube/Polymer Composite Thin Films for Energy Conversion. *ACS Nano* **2012**, *6*, 1347–1356.
41. Landi, B. J.; Cress, C. D.; Raffaelle, R. P. High Energy Density Lithium-Ion Batteries with Carbon Nanotube Anodes. *J. Mater. Res.* **2010**, *25*, 1636–1644.
42. Landi, B. J.; Ganter, M. J.; Schauerman, C. M.; Cress, C. D.; Raffaelle, R. P. Lithium Ion Capacity of Single Wall Carbon

Nanotube Paper Electrodes. *J. Phys. Chem. C* **2008**, *112*, 7509–7515.
43. Oh, J.-M.; Geiculescu, O.; DesMarteau, D.; Creager, S. Ionomer Binders Can Improve Discharge Rate Capability in Lithium-Ion Battery Cathodes. *J. Electrochem. Soc.* **2011**, *158*, A207–A213.
44. Liang, H.-Y.; Qiu, X.-P.; Zhang, S.-C.; Zhu, W.-T.; Chen, L.-Q. Study of Lithiated Nafion Ionomer for Lithium Batteries. *J. Appl. Electrochem.* **2004**, *34*, 1211–1214.
45. Delongchamp, D. M.; Hammond, P. T. Fast Ion Conduction in Layer-by-Layer Polymer Films. *Chem. Mater.* **2003**, *15*, 1165–1173.
46. Cheung, J. H.; Stockton, W. B.; Rubner, M. F. Molecular-Level Processing of Conjugated Polymers. 3. Layer-by-Layer Manipulation of Polyaniline via Electrostatic Interactions. *Macromolecules* **1997**, *30*, 2712–2716.